CellPress

Cell Metabolism
Short Article

FGF21 Acts Centrally to Induce Sympathetic Nerve Activity, Energy Expenditure, and Weight Loss

Bryn M. Owen,[1,6] Xunshan Ding,[1,2,5,6] Donald A. Morgan,[3] Katie Colbert Coate,[1,4] Angie L. Bookout,[1] Kamal Rahmouni,[3] Steven A. Kliewer,[1,2,*] and David J. Mangelsdorf[1,4,*]

[1]Department of Pharmacology, University of Texas Southwestern Medical Center, Dallas, TX 75390, USA
[2]Department of Molecular Biology, University of Texas Southwestern Medical Center, Dallas, TX 75390, USA
[3]Department of Pharmacology, University of Iowa Carver College of Medicine, Iowa City, IA 52242, USA
[4]Howard Hughes Medical Institute, University of Texas Southwestern Medical Center, Dallas, TX 75390, USA
[5]Current address: NGM Biopharmaceuticals, South San Francisco, CA 94080, USA
[6]Co-first author
*Correspondence: steven.kliewer@utsouthwestern.edu (S.A.K.), davo.mango@utsouthwestern.edu (D.J.M.)
http://dx.doi.org/10.1016/j.cmet.2014.07.012

SUMMARY

The mechanism by which pharmacologic administration of the hormone FGF21 increases energy expenditure to cause weight loss in obese animals is unknown. Here we report that FGF21 acts centrally to exert its effects on energy expenditure and body weight in obese mice. Using tissue-specific knockout mice, we show that βKlotho, the obligate coreceptor for FGF21, is required in the nervous system for these effects. FGF21 stimulates sympathetic nerve activity to brown adipose tissue through a mechanism that depends on the neuropeptide corticotropin-releasing factor. Our findings provide an unexpected mechanistic explanation for the strong pharmacologic effects of FGF21 on energy expenditure and weight loss in obese animals.

INTRODUCTION

FGF21 is a hormone expressed in liver, where it is induced by states of nutrient stress, including starvation and ketogenic or high-carbohydrate diets, and the fibrate drugs. FGF21 is also expressed in white adipose tissue (WAT), where it is induced by fasting/refeeding regimens and the thiazolidinedione drugs, and in brown adipose tissue (BAT), where it is induced by cold (reviewed in Potthoff et al., 2012). In rodent models of obesity, FGF21 administration caused weight loss by increasing energy expenditure and improved insulin sensitivity and lipid parameters (Coskun et al., 2008; Kharitonenkov et al., 2005; Xu et al., 2009a, 2009b). Similar metabolic effects were seen in diabetic rhesus monkeys and patients with type 2 diabetes (Gaich et al., 2013; Kharitonenkov et al., 2007; Véniant et al., 2012b).

FGF21 acts through a cell surface receptor comprised of an FGF receptor (FGFR), with FGFR1c the preferred isoform, in complex with βKlotho (reviewed in Potthoff et al., 2012). While the FGFRs are broadly expressed, βKlotho is expressed in a more limited set of tissues, including WAT, BAT, and liver (Fon Tacer et al., 2010). FGF21 mediates its pharmacologic effects on body weight and insulin sensitivity in part through WAT and BAT (Adams et al., 2012; Ding et al., 2012; Véniant et al., 2012a; Wu et al., 2011), where it induces uncoupling protein-1 (*Ucp1*) and uncoupled respiration (Fisher et al., 2012; Hondares et al., 2010) and the hormone adiponectin (Holland et al., 2013; Lin et al., 2013). FGF21 also acts on the nervous system. FGF21 is not expressed in the CNS (Fon Tacer et al., 2010) but crosses the blood-brain barrier (Hsuchou et al., 2007) and is present in human cerebrospinal fluid (Tan et al., 2011). Intracerebroventricular (i.c.v.) injection of FGF21 increased metabolic rate and insulin sensitivity in rats (Sarruf et al., 2010). Within the nervous system, βKlotho is expressed in the suprachiasmatic nucleus (SCN) in the hypothalamus. It is also expressed in the area postrema, nucleus of the solitary tract, and nodose ganglia, which are discrete anatomical nuclei that together comprise the dorsal-vagal complex (DVC) (Bookout et al., 2013). Using lean mice specifically lacking βKlotho in the hypothalamus and/or the hindbrain, we showed that βKlotho in the hypothalamus is required for FGF21 to increase circulating ketone body and glucocorticoid concentrations, to suppress growth and female reproduction, and to modulate circadian behavior (Bookout et al., 2013; Owen et al., 2013). However, since these studies were all done in lean mice, they did not address whether the effects of FGF21 on energy expenditure require that it act on the nervous system. In this paper, we examine the contribution of the nervous system to the pharmacologic actions of FGF21 in the context of diet-induced obesity (DIO).

RESULTS AND DISCUSSION

FGF21 Acts Centrally to Induce Energy Expenditure

Fgf21-transgenic (Tg) mice are resistant to weight gain (Ding et al., 2012; Kharitonenkov et al., 2005). To determine whether this effect involves FGF21 acting in the brain, we crossed Klb^{Camk2a} mice, in which the βKlotho gene (*Klb*) is disrupted in both the hypothalamus (including the SCN) and DVC, but not in adipose tissue and liver (Bookout et al., 2013), with *Fgf21*-Tg mice to generate four genotypes: $Klb^{fl/fl}$, $Klb^{fl/fl}$/Tg, Klb^{Camk2a}, and Klb^{Camk2a}/Tg mice. As expected (Inagaki et al., 2008), $Klb^{fl/fl}$/Tg mice weighed less than $Klb^{fl/fl}$ mice on the standard chow diet due to their smaller body size, and this effect was

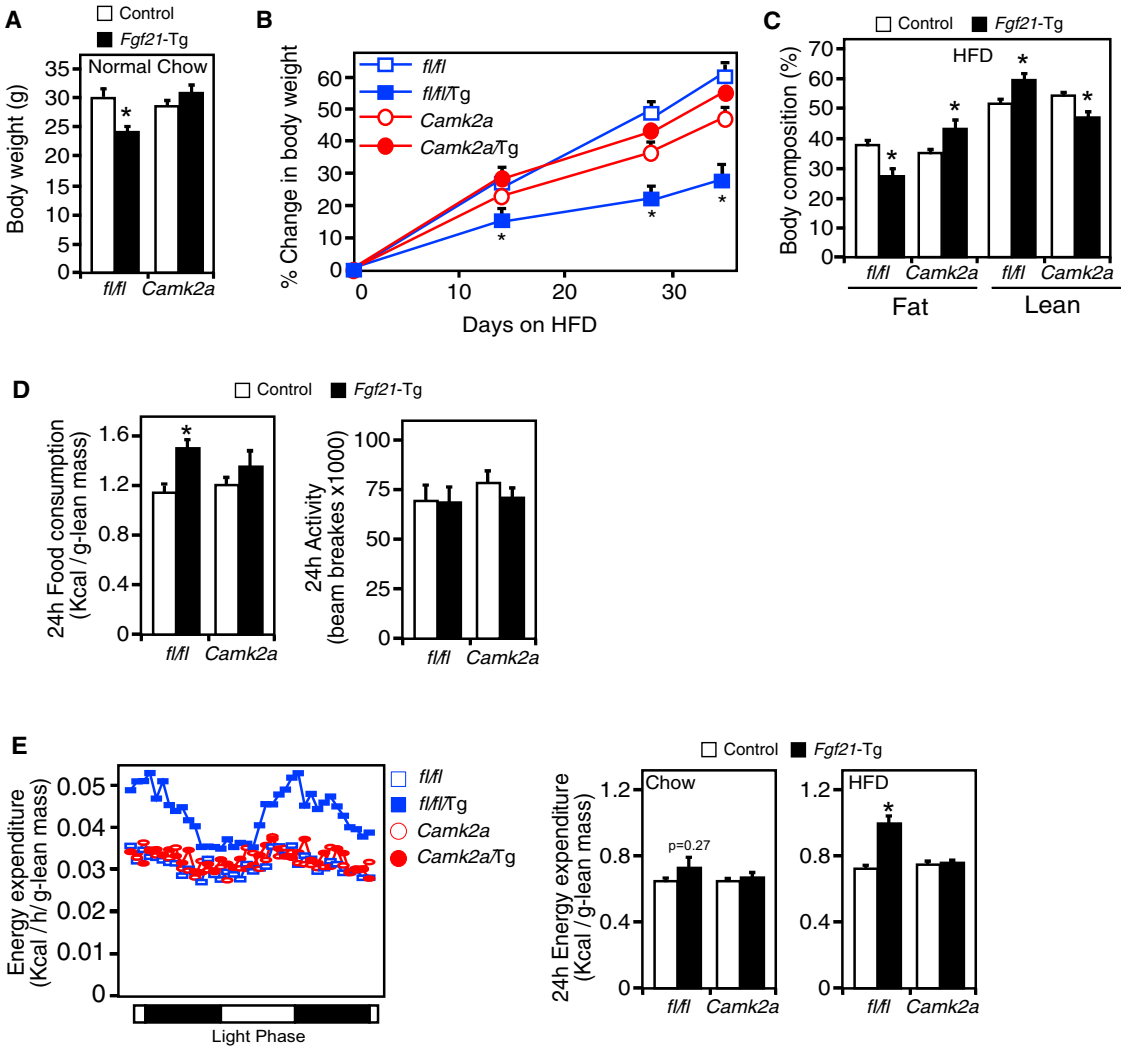

Figure 1. *Klb* Expression in the Nervous System Is Required for the Effects of FGF21 on Whole-Body Energy Expenditure

(A) Body weight in chow-fed groups of $Klb^{fl/fl}$, $Klb^{fl/fl}$/Tg, Klb^{Camk2a}, and Klb^{Camk2a}/Tg mice.

(B) Percent change in body weight in groups of mice fed a high-fat diet (HFD). Body weights for the groups at the end of the study were as follows (in grams): $Klb^{fl/fl}$, 44 ± 2.5; $Klb^{fl/fl}$/Tg, 33 ± 1.7; Klb^{Camk2a}, 40 ± 1.3; Klb^{Camk2a}/Tg, 47 ± 2.6.

(C) Body composition after 8 weeks on HFD.

(D) Food consumption (normalized to body weight) and physical activity during a 24 hr period while on a HFD.

(E) Left: energy expenditure starting 24 hr after switching mice to the HFD. Right: quantification of 24 hr energy expenditure data for the same mice on either regular chow or HFD.

(A)–(C) were performed with mice housed at 22°–23°. (D) and (E) were performed using metabolic cages maintained at 21°–22°.

Data are shown as the mean ± SEM. n = 8–13/group (A–C); n = 6/group (D and E). *p < 0.05 compared to control.

absent in Klb^{Camk2a}/Tg mice (Figure 1A). When fed a high-fat diet (HFD), $Klb^{fl/fl}$/Tg mice gained less weight than $Klb^{fl/fl}$ and Klb^{Camk2a} mice (Figure 1B). These effects of FGF21 overexpression were lost in the Klb^{Camk2a}/Tg mice (Figure 1B). HFD-fed $Klb^{fl/fl}$/Tg mice had a reduced percentage of fat mass and plasma leptin concentrations and increased percentage of lean mass compared to the other three genotypes (Figure 1C; Table S1, available online). In metabolic cage studies, the $Klb^{fl/fl}$/Tg mice had significantly increased food consumption and energy expenditure with no change in physical activity (Figures 1D and 1E). This significant effect of FGF21 on energy expenditure was not observed in the same mice fed a regular chow diet (Figure 1E), suggesting that oxidative substrate was limiting. Together, these data demonstrate that in the context of nutritional surfeit, FGF21 acts on the nervous system to stimulate energy expenditure.

We further evaluated carbohydrate and lipid parameters in the HFD-fed $Klb^{fl/fl}$, $Klb^{fl/fl}$/Tg, Klb^{Camk2a}, and Klb^{Camk2a}/Tg mice. Plasma glucose, insulin, and cholesterol were all significantly lower in $Klb^{fl/fl}$/Tg mice than in the other three genotypes, and plasma triglycerides showed a similar trend (Table S1). Likewise, hepatic cholesterol and triglyceride concentrations were significantly lower in $Klb^{fl/fl}$/Tg mice than in the other genotypes (Table S1).

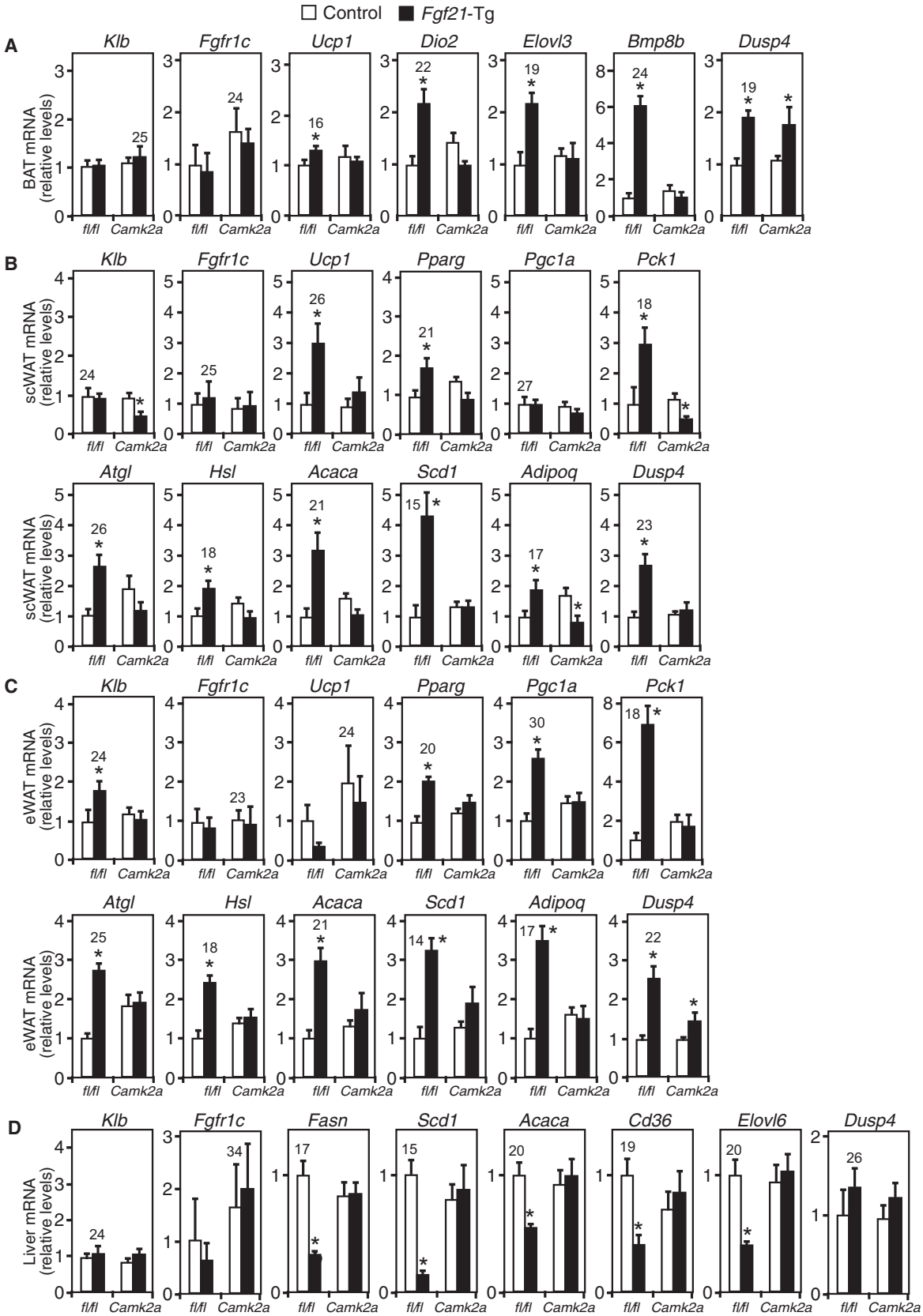

(legend on next page)

FGF21 Acts Centrally to Induce Thermogenic Genes

We next compared gene expression in BAT, subcutaneous (sc) and epididymal (e) WAT and liver of *Klb*$^{fl/fl}$, *Klb*$^{fl/fl}$/Tg, *Klb*^{Camk2a}, and *Klb*^{Camk2a}/Tg mice. As expected, *Klb* was unchanged in BAT, scWAT, eWAT, and liver of *Klb*^{Camk2a} compared to *Klb*$^{fl/fl}$ mice, although FGF21 overexpression increased *Klb* mRNA in eWAT in *Klb*$^{fl/fl}$, but not *Klb*^{Camk2a}, mice (Figures 2A–2D). There were no differences among genotypes in *Fgfr1c* expression. In BAT, *Ucp1*, deiodinase 2 (*Dio2*), and elongation of very long chain fatty acids like 3 (*Elovl3*) were elevated in *Klb*$^{fl/fl}$/Tg compared to *Klb*$^{fl/fl}$ mice, consistent with increased thermogenesis (Figure 2A). Interestingly, bone morphogenic protein 8b (*Bmp8b*), which is induced in BAT in response to cold or HFD feeding and sensitizes BAT to the thermogenic actions of norepinephrine (Whittle et al., 2012), was increased markedly in *Klb*$^{fl/fl}$/Tg mice compared to *Klb*$^{fl/fl}$ controls (Figure 2A). In scWAT, *Ucp1*, peroxisome proliferator-activated receptor γ (*Pparg*), phosphoenolpyruvate carboxykinase (*Pck1*), adipocyte triacylglycerol lipase (*Atgl*), hormone-sensitive lipase (*Hsl*), acetyl-CoA carboxylase α (*Acaca*), stearoyl-coenzyme A desaturase 1 (*Scd1*), and adiponectin (*Adipoq*) were increased in *Klb*$^{fl/fl}$/Tg compared to *Klb*$^{fl/fl}$ controls (Figure 2B). The induction of *Ucp1* is consistent with a recent report showing that FGF21 causes browning of WAT (Fisher et al., 2012). In eWAT, *Pparg*, PPARγ coactivator-1α (*Pgc1a*), *Pck1*, *Atgl*, *Hsl*, *Acaca*, *Scd1*, and *Adipoq* were increased in *Klb*$^{fl/fl}$/Tg compared to *Klb*$^{fl/fl}$ mice (Figure 2C). All of these FGF21-dependent changes in gene expression were lost in *Klb*^{Camk2a}/Tg mice (Figures 2A–2C), demonstrating that βKlotho in the nervous system is important for FGF21 to exert many of its pharmacologic effects on gene expression in adipose tissue. Since FGF21 also acts directly on adipocytes to induce *Ucp1* and other genes (Fisher et al., 2012; Hondares et al., 2010), their maximal induction likely involves cooperative effects of FGF21 on both adipose tissue and the nervous system. In liver, fatty acid synthase (*Fasn*), *Scd1*, *Acaca*, *Cd36*, and *Elovl6* were decreased in *Klb*$^{fl/fl}$/Tg compared to *Klb*$^{fl/fl}$ mice (Figure 2D). These inhibitory effects of FGF21 were also absent in *Klb*^{Camk2a}/Tg mice (Figure 2D). A recent study showed that the effects of FGF21 on reducing triglyceride and cholesterol concentrations were lost in liver-specific insulin receptor knockout mice (Emanuelli et al., 2014). Similarly, the loss of FGF21 action in liver of *Klb*^{Camk2a}/Tg mice may be secondary to the loss of its insulin-lowering action (Table S1). Expression of dual specificity phosphatase 4 (*Dusp4*), which inhibits ERK1/2, was increased in *Klb*$^{fl/fl}$/Tg mice compared to *Klb*$^{fl/fl}$ mice in all three adipose tissue depots, but not liver (Figures 2A–2D). *Dusp4* was still increased in *Klb*^{Camk2a}/Tg compared to *Klb*^{Camk2a} mice in BAT and eWAT (Figures 2A and 2C), reinforcing the notion that FGF21 can also act directly on adipose tissue.

FGF21 Acts on the Hypothalamus

To assess the relative contribution of βKlotho in the DVC versus the hypothalamus to the metabolic actions of FGF21, we crossed *Fgf21*-Tg mice with *Klb*^{Phox2b} mice, in which *Klb* is disrupted in the DVC but not the hypothalamus (Bookout et al., 2013). Metabolic parameters were evaluated in HFD-fed *Klb*$^{fl/fl}$, *Klb*$^{fl/fl}$/Tg, *Klb*^{Phox2b}, and *Klb*^{Phox2b}/Tg mice. In contrast to *Klb*^{Camk2a}/Tg mice, *Klb*^{Phox2b}/Tg mice were similar to *Klb*$^{fl/fl}$/Tg mice with respect to weight gain, energy expenditure, and plasma insulin and glucose concentrations, although the significance of the decrease in glucose was lost in the *Klb*^{Phox2b}/Tg mice (Figure S1A). Likewise, *Klb*^{Phox2b}/Tg and *Klb*$^{fl/fl}$/Tg mice had comparable changes in the expression of *Ucp1* in BAT (Figure S1B). However, the significance of *Ucp1* induction in scWAT was lost in the *Klb*^{Phox2b}/Tg mice (Figure S1B). Overall, these data support the importance of βKlotho in the hypothalamus and not the DVC for the central actions of FGF21.

Since *Fgf21*-Tg mice are chronically exposed to high levels of FGF21, we examined whether the metabolic effects of shorter-term exposure to recombinant FGF21 in DIO mice also require βKlotho in the nervous system. DIO *Klb*$^{fl/fl}$ and *Klb*^{Camk2a} mice were administered FGF21 or vehicle for 2 weeks by osmotic minipump. Plasma FGF21 concentrations were 29 ± 11 ng/ml and 36 ± 13 ng/ml in the *Klb*$^{fl/fl}$ and *Klb*^{Camk2a} mice, respectively. As expected, FGF21 decreased body weight, percent body fat, and plasma insulin, glucose, cholesterol, and leptin concentrations in DIO *Klb*$^{fl/fl}$ mice (Figure 3A). All of these effects of FGF21 were absent in the *Klb*^{Camk2a} mice (Figure 3A). FGF21 administration also increased *Ucp1* expression in BAT and scWAT in *Klb*$^{fl/fl}$, but not *Klb*^{Camk2a}, mice (Figure 3B). Overall, the pattern of gene expression in BAT, scWAT, eWAT, and liver of *Klb*$^{fl/fl}$ and *Klb*^{Camk2a} mice in response to recombinant FGF21 was similar to that seen with the FGF21 transgene, with nearly all of the effects of FGF21 lost in the *Klb*^{Camk2a} background (Figure S2). Thus, βKlotho in the nervous system is required for the pharmacologic actions of FGF21 in DIO mice.

FGF21 Induces Sympathetic Nerve Activity

Since BAT-mediated energy expenditure is regulated by the sympathetic nervous system, we used multifiber sympathetic nerve recording to directly measure the effect of FGF21 on sympathetic nerve activity (SNA) subserving BAT in mice. Injection of FGF21 i.c.v. increased BAT SNA in a time- and dose-dependent manner (Figures 4A and 4B). SNA was induced approximately 30 min after FGF21 administration and continued to increase over the 4 hr experiment. This effect was blocked by i.c.v. pretreatment with PD173074 (Figure 4B), which inhibits the tyrosine kinase activities of FGFR1, FGFR2, and FGFR3 (Kunii et al., 2008; Mohammadi et al., 1998). Intravenous (i.v.) injection of FGF21 also increased BAT SNA, which was inhibited by i.c.v. pretreatment with PD173074 (Figure 4C). The onset of SNA induction was slower after i.v. injection compared to i.c.v. injection, as expected, since FGF21 must cross the blood-brain barrier. The effect of FGF21 on SNA when administered peripherally was

Figure 2. *Klb* Expression in the Nervous System Is Required for the Effects of FGF21 on Gene Expression in HFD-Fed Mice

(A–D) Gene expression was analyzed by qPCR in (A) brown adipose tissue (BAT), (B) subcutaneous (sc) white adipose tissue (WAT), (C) epididymal (e) WAT, and (D) liver of *Klb*$^{fl/fl}$, *Klb*$^{fl/fl}$/Tg, *Klb*^{Camk2a}, and *Klb*^{Camk2a}/Tg mice after 3 months on the high-fat diet. qPCR cycle time values are shown for the group with highest expression for each gene. Data are shown as the mean ± SEM. n = 8–13/group. *$p < 0.05$ compared to control.

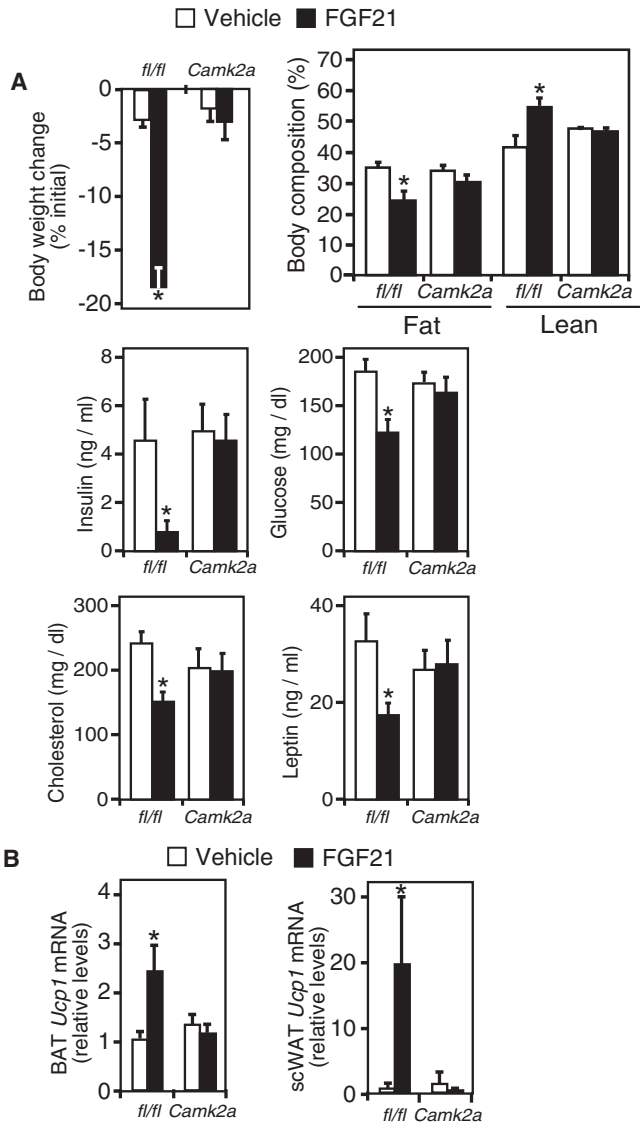

Figure 3. *Klb* Expression in the Nervous System Is Required for Metabolic Actions of Recombinant FGF21 Delivered by Minipump

(A and B) Groups of diet-induced obese mice were administered FGF21 (0.8 mg/kg/day) or vehicle by osmotic minipump for 2 weeks and evaluated for (A) percent change in body weight (day 1 versus day 14), body composition, and plasma insulin, glucose, cholesterol, and leptin concentrations (day 14) or (B) uncoupling protein-1 (*Ucp1*) gene expression in brown adipose tissue (BAT) and subcutaneous white adipose tissue (scWAT). For (A), body weights for the groups at the end of the study were as follows (in grams): $Klb^{fl/fl}$/vehicle, 34 ± 1.3; $Klb^{fl/fl}$/FGF21, 30 ± 1.0; Klb^{Camk2a}/vehicle, 36 ± 1.6; Klb^{Camk2a}/FGF21, 36 ± 1.3. Data are shown as the mean ± SEM. n = 5–6/group. *p < 0.05 compared to vehicle.

markedly attenuated in Klb^{Camk2a} mice (Figure 4D). The residual effect of FGF21 on BAT SNA in the Klb^{Camk2a} mice could be due to either incomplete knockout of βKlotho in the nervous system or FGF21 acting via other, unknown mechanisms. Regardless, the data in Figure 1E show that βKlotho in the nervous system is crucial for the effect of FGF21 on energy expenditure.

FGF21 Actions Require Corticotropin-Releasing Factor

We previously showed that corticotropin-releasing factor (*Crf*) mRNA in hypothalamus and circulating corticosterone concentrations are increased in *Fgf21*-Tg mice (Bookout et al., 2013). Likewise, hypothalamic *Crf* mRNA was elevated 3 hr after intraperitoneal injection of FGF21, and there was a corresponding increase in plasma adrenocorticotropic hormone (ACTH) (Figure 4E). While ACTH concentrations were increased under these acute FGF21 treatment conditions, they were reduced after administration of FGF21 for 2 weeks and in *Fgf21*-Tg mice (Bookout et al., 2013), suggesting that chronic FGF21 exposure sensitizes the adrenal to ACTH. Indeed, there is evidence that the autonomic nervous system can modulate the sensitivity of the adrenal to ACTH (Kalsbeek et al., 2010). Since i.c.v. injection of CRF stimulates sympathetic outflow to BAT and thermogenesis in rats (Arase et al., 1988; Cerri and Morrison, 2006; LeFeuvre et al., 1987), we tested whether CRF contributes to the effects of FGF21 on BAT. Notably, i.c.v. injection of the CRF receptor antagonist, α-helical CRF(9-41) (Rivier et al., 1986), which inhibits both the CRF1 and CRF2 receptor subtypes, completely blocked the effect of FGF21 on SNA in BAT (Figure 4F). This finding that FGF21 action involves downstream effects on CRF likely explains the relatively slow onset of SNA in BAT in response to FGF21. In the hypothalamus, βKlotho is most highly expressed in the SCN, whereas CRF is primarily localized in the paraventricular nucleus (PVN). Since the SCN is known to act on the PVN to regulate the circadian pattern of CRF and corticosterone release (Kalsbeek et al., 2010), FGF21 may mediate its effects on CRF indirectly via the SCN. However, the precise neuroanatomical relationship between βKlotho and CRF remains to be determined. Nevertheless, our findings suggest that FGF21 regulates both BAT SNA and corticosterone levels via its effects on CRF.

In summary, we demonstrate that FGF21 acts centrally to stimulate sympathetic outflow, energy expenditure, and weight loss in DIO mice. We previously showed that the acute effects of FGF21 on whole-body insulin sensitivity and glucose uptake in BAT were lost in HFD-fed mice lacking βKlotho in adipose tissue (Ding et al., 2012). How do we reconcile these findings? In vivo, the thermogenic effects of UCP1 require both norepinephrine and oxidative substrate (Nedergaard et al., 2005). For example, while PPARγ agonists efficiently stimulate *Ucp1* expression and lipid accumulation in both brown and white adipocytes, they do not increase thermogenesis. However, they potentiate the thermogenic actions of β-adrenergic receptor agonists (Foellmi-Adams et al., 1996; Sell et al., 2004; Thurlby et al., 1987). We suggest that FGF21 works similarly to this combination of PPARγ and β-adrenergic receptor agonists through a 2-fold mechanism (Figure 4G). First, FGF21 acts on the nervous system to stimulate sympathetic outflow to BAT, which induces *Ucp1* and lipolysis (Cannon and Nedergaard, 2004). FGF21 also promotes the browning of scWAT (Fisher et al., 2012), an effect that in vivo involves βKlotho in the nervous system. Second, FGF21 acts directly on BAT and scWAT to increase glucose uptake and substrate mobilization. Accordingly, we find that energy expenditure is markedly upregulated in lean *Fgf21*-Tg mice when they are switched to the HFD and additional substrate is made available for oxidation (Figure 1E). Thus, FGF21 regulates both the mobilization and uncoupled oxidation of substrate in BAT and browned WAT.

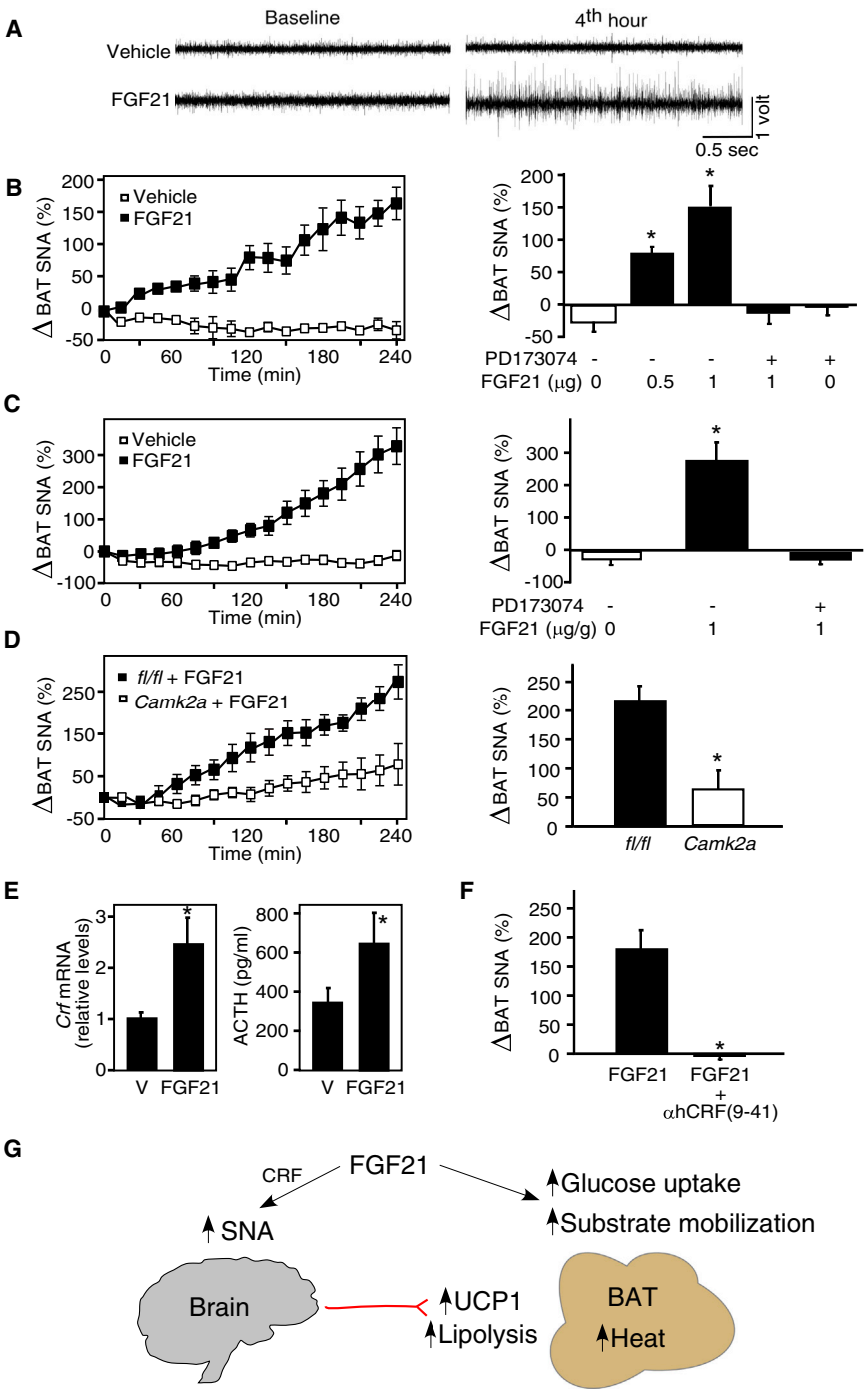

Figure 4. FGF21 Acts Centrally to Stimulate Brown Adipose Tissue Sympathetic Nerve Activity

(A) Representative sympathetic nerve activity (SNA) recordings at baseline and 4 hr after intracerebroventricular (i.c.v.) administration of FGF21 (1 μg) or vehicle.

(B) Left: percent change in BAT SNA following i.c.v. injection of FGF21 (1 μg) or vehicle. Right: percent change in BAT SNA at 3–4 hr following i.c.v. injection of FGF21 at the indicated doses. Mice were pretreated for 10 min with either vehicle or an FGF receptor inhibitor (PD173074, 25 μg) delivered i.c.v. as indicated.

(C) Left: percent change in BAT SNA following intravenous (i.v.) injection of vehicle or FGF21 (1 mg/kg). Right: percent change in BAT SNA at 3–4 hr following i.v. injection of FGF21. Mice were pretreated for 10 min with either PD173074 or vehicle delivered i.c.v. as indicated.

(D) Left: percent change in BAT SNA following i.v. injection of FGF21 (1 mg/kg) into *Klb*$^{fl/fl}$ or *Klb*^{Camk2a} mice. Right: quantification of SNA data at the 3–4 hr time points.

(E) *Crf* mRNA levels in whole hypothalamus and plasma adrenocorticotropic hormone (ACTH) concentrations 3 hr after i.p. injection with either vehicle or FGF21 (1 mg/kg).

(F) Percent change in BAT SNA 3–4 hr after i.c.v. injection of FGF21 (1 μg). Mice were pretreated for 10 min with either vehicle (saline, 2 μl) or α-helical CRF(9-41) (αhCRF(9-41); 6 μg) delivered i.c.v. as indicated.

Data are shown as the mean ± SEM. n = 5–7/group. *p < 0.05 compared to either vehicle (B, C, and E) or *Klb*$^{fl/fl}$ (D) as determined by t test. For (B)–(D) (right panels) and (F), the percent change in BAT SNA was calculated based on the average of the final four time points relative to baseline.

(G) Model for the effects of FGF21 on energy expenditure. FGF21 acts on the hypothalamus to induce corticotropin-releasing factor (CRF) and to stimulate sympathetic nerve activity (SNA), which in turn induces uncoupling protein-1 (UCP1) and lipolysis in brown adipose tissue (BAT). FGF21 also acts directly on BAT to stimulate glucose uptake and to mobilize oxidative substrate. These dual effects induce efficient energy expenditure. The model is based on this study and previous literature (Cannon and Nedergaard, 2004; Ding et al., 2012).

EXPERIMENTAL PROCEDURES

Mouse Studies

Mouse strains have been described and are on mixed C57BL6J;129/Sv backgrounds (Bookout et al., 2013; Owen et al., 2013). Age-matched 3- to 7-month-old male littermates were used for all experiments and were fed either a standard chow (Harlan Teklad, TD.2916) or a high-fat diet containing 60% fat (Research Diets, D12492i). For the minipump experiments, mice were maintained on the high-fat diet for 12 weeks prior to initiating the experiment. Housing rooms were maintained between 22°C and 23°C. Metabolic cage studies were performed at 21°C–22°C. Indirect calorimetry using LabMaster metabolic cages (TSE Systems) was used to determine energy expenditure per gram of lean body mass. Energy expenditure was calculated as a function of O_2 consumption and CO_2 production according the following formula: energy expenditure (kcal/hr) = ((3.941 × vO_2 (ml/hr)) + (1.106 × vCO_2 (ml/hr)))/1,000. Body composition was measured using an EchoMRI-100 Body Composition Analyzer. All experiments were approved by the Institutional Animal Care and Research Advisory Committee of the University of Texas Southwestern Medical Center or the University of Iowa.

Materials

Recombinant human FGF21 was from Novo Nordisk. Subcutaneous osmotic pumps were from ALZET. PD173074 was from Sigma. α-helical CRF(9-41) was from Phoenix Pharmaceuticals. The following kits were used to measure

metabolic parameters: glucose (Wako Chemicals), triglycerides (Wako Chemicals), cholesterol (Fisher Scientific), insulin (Crystal Chem), leptin (Linco), and adrenocorticotropic hormone. Liver triglyceride and cholesterol levels were measured as described (Zhang et al., 2012).

Real-Time Quantitative PCR Analyses

Total RNA was extracted from liver using Stat 60 reagent (IsoTex Diagnostics). For adipose tissue, RNeasy lipid tissue mini kits (QIAGEN) were used. RNA (1–2 μg) from each sample was then used to generate cDNA (Invitrogen). qPCR was performed using SYBR green as described (Bookout et al., 2006).

Sympathetic Nerve Activity Measurements

Measurement of sympathetic nerve activity to BAT was performed as described (Harlan et al., 2011; Lockie et al., 2012; Morgan and Rahmouni, 2010). Following the establishment of baseline values, mice were pretreated for 10 min with either vehicle (10 mM Na_2HPO_4, 2% [w/v] glycerol [pH 7.6]), PD173074, or α-helical CRF(9-41) administered i.c.v. followed by i.c.v. or i.v. (jugular vein infusion) administration of vehicle (10 mM Na_2HPO_4, 2% [w/v] glycerol [pH 7.6]) or recombinant FGF21. SNA was recorded for an additional 4 hr. All i.c.v. injection volumes were 2 μl. The dose of PD173074 used (25 μg), which had no effect on SNA on its own (Figure 4B), was based on a previous publication in which PD173074 inhibited FGF19 action (Morton et al., 2013). The dose of α-helical CRF(9-41) (6 μg) was based on a previous publication in which this CRF antagonist blocked SNA activity in rats (Correia et al., 2001).

Statistical Analyses

Statistical analyses were performed by two-way ANOVA with post hoc correction (GraphPad Prism) unless indicated otherwise. Data are presented as the mean ± SEM; $p < 0.05$ was considered significant.

SUPPLEMENTAL INFORMATION

Supplemental Information includes two figures and one table and can be found with this article online at http://dx.doi.org/10.1016/j.cmet.2014.07.012.

AUTHOR CONTRIBUTIONS

B.M.O. designed, conducted, and analyzed experiments involving *Klb*^{Phox2b} mice, osmotic minipumps, and FGF21 injection. X.D. initiated the project and designed, conducted, and analyzed experiments involving *Klb*^{Camk2a} and *Klb*^{Phox2b} mice. D.A.M. and K.R. designed, conducted, and analyzed the sympathetic nerve activity experiments. K.C.C. contributed to gene expression analyses and project design, and A.L.B. contributed to project design. S.A.K. and D.J.M. supervised the project and wrote the paper.

ACKNOWLEDGMENTS

We thank Yuan Zhang, Heather Lawrence, Kevin Vale, and Sofya Perelman for technical assistance and Birgitte Andersen (Novo Nordisk) for providing human recombinant FGF21. This work was supported by National Institutes of Health grants R01DK067158 (S.A.K. and D.J.M.), 1F32DK098908 (K.C.C), GM007062 (A.L.B.), and HL084207 (K.R.); the Robert A. Welch Foundation (grant I-1558 to S.A.K. and grant I-1275 to D.J.M.); the American Heart Association (14EIA18860041 to K.R.); and the Howard Hughes Medical Institute (to K.C.C. and D.J.M.). X.D. is an employee and stockholder of NGM Biopharmaceuticals. The recombinant FGF21 was provided by Novo Nordisk.

Received: February 19, 2014
Revised: June 2, 2014
Accepted: July 15, 2014
Published: August 14, 2014

REFERENCES

Adams, A.C., Yang, C., Coskun, T., Cheng, C.C., Gimeno, R.E., Luo, Y., and Kharitonenkov, A. (2012). The breadth of FGF21's metabolic actions are governed by FGFR1 in adipose tissue. Mol Metab *2*, 31–37.

Arase, K., York, D.A., Shimizu, H., Shargill, N., and Bray, G.A. (1988). Effects of corticotropin-releasing factor on food intake and brown adipose tissue thermogenesis in rats. Am. J. Physiol. *255*, E255–E259.

Bookout, A.L., Cummins, C.L., Mangelsdorf, D.J., Pesola, J.M., and Kramer, M.F. (2006). High-throughput real-time quantitative reverse transcription PCR. Curr. Protoc. Mol. Biol. *Chapter 15*, 8.

Bookout, A.L., de Groot, M.H., Owen, B.M., Lee, S., Gautron, L., Lawrence, H.L., Ding, X., Elmquist, J.K., Takahashi, J.S., Mangelsdorf, D.J., and Kliewer, S.A. (2013). FGF21 regulates metabolism and circadian behavior by acting on the nervous system. Nat. Med. *19*, 1147–1152.

Cannon, B., and Nedergaard, J. (2004). Brown adipose tissue: function and physiological significance. Physiol. Rev. *84*, 277–359.

Cerri, M., and Morrison, S.F. (2006). Corticotropin releasing factor increases in brown adipose tissue thermogenesis and heart rate through dorsomedial hypothalamus and medullary raphe pallidus. Neuroscience *140*, 711–721.

Correia, M.L., Morgan, D.A., Mitchell, J.L., Sivitz, W.I., Mark, A.L., and Haynes, W.G. (2001). Role of corticotrophin-releasing factor in effects of leptin on sympathetic nerve activity and arterial pressure. Hypertension *38*, 384–388.

Coskun, T., Bina, H.A., Schneider, M.A., Dunbar, J.D., Hu, C.C., Chen, Y., Moller, D.E., and Kharitonenkov, A. (2008). Fibroblast growth factor 21 corrects obesity in mice. Endocrinology *149*, 6018–6027.

Ding, X., Boney-Montoya, J., Owen, B.M., Bookout, A.L., Coate, K.C., Mangelsdorf, D.J., and Kliewer, S.A. (2012). βKlotho is required for fibroblast growth factor 21 effects on growth and metabolism. Cell Metab. *16*, 387–393.

Emanuelli, B., Vienberg, S.G., Smyth, G., Cheng, C., Stanford, K.I., Arumugam, M., Michael, M.D., Adams, A.C., Kharitonenkov, A., and Kahn, C.R. (2014). Interplay between FGF21 and insulin action in the liver regulates metabolism. J. Clin. Invest. *124*, 515–527.

Fisher, F.M., Kleiner, S., Douris, N., Fox, E.C., Mepani, R.J., Verdeguer, F., Wu, J., Kharitonenkov, A., Flier, J.S., Maratos-Flier, E., and Spiegelman, B.M. (2012). FGF21 regulates PGC-1α and browning of white adipose tissues in adaptive thermogenesis. Genes Dev. *26*, 271–281.

Foellmi-Adams, L.A., Wyse, B.M., Herron, D., Nedergaard, J., and Kletzien, R.F. (1996). Induction of uncoupling protein in brown adipose tissue. Synergy between norepinephrine and pioglitazone, an insulin-sensitizing agent. Biochem. Pharmacol. *52*, 693–701.

Fon Tacer, K., Bookout, A.L., Ding, X., Kurosu, H., John, G.B., Wang, L., Goetz, R., Mohammadi, M., Kuro-o, M., Mangelsdorf, D.J., and Kliewer, S.A. (2010). Research resource: Comprehensive expression atlas of the fibroblast growth factor system in adult mouse. Mol. Endocrinol. *24*, 2050–2064.

Gaich, G., Chien, J.Y., Fu, H., Glass, L.C., Deeg, M.A., Holland, W.L., Kharitonenkov, A., Bumol, T., Schilske, H.K., and Moller, D.E. (2013). The effects of LY2405319, an FGF21 analog, in obese human subjects with type 2 diabetes. Cell Metab. *18*, 333–340.

Harlan, S.M., Morgan, D.A., Agassandian, K., Guo, D.F., Cassell, M.D., Sigmund, C.D., Mark, A.L., and Rahmouni, K. (2011). Ablation of the leptin receptor in the hypothalamic arcuate nucleus abrogates leptin-induced sympathetic activation. Circ. Res. *108*, 808–812.

Holland, W.L., Adams, A.C., Brozinick, J.T., Bui, H.H., Miyauchi, Y., Kusminski, C.M., Bauer, S.M., Wade, M., Singhal, E., Cheng, C.C., et al. (2013). An FGF21-adiponectin-ceramide axis controls energy expenditure and insulin action in mice. Cell Metab. *17*, 790–797.

Hondares, E., Rosell, M., Gonzalez, F.J., Giralt, M., Iglesias, R., and Villarroya, F. (2010). Hepatic FGF21 expression is induced at birth via PPARalpha in response to milk intake and contributes to thermogenic activation of neonatal brown fat. Cell Metab. *11*, 206–212.

Hsuchou, H., Pan, W., and Kastin, A.J. (2007). The fasting polypeptide FGF21 can enter brain from blood. Peptides *28*, 2382–2386.

Inagaki, T., Lin, V.Y., Goetz, R., Mohammadi, M., Mangelsdorf, D.J., and Kliewer, S.A. (2008). Inhibition of growth hormone signaling by the fasting-induced hormone FGF21. Cell Metab. *8*, 77–83.

Kalsbeek, A., Fliers, E., Hofman, M.A., Swaab, D.F., and Buijs, R.M. (2010). Vasopressin and the output of the hypothalamic biological clock. J. Neuroendocrinol. *22*, 362–372.

Kharitonenkov, A., Shiyanova, T.L., Koester, A., Ford, A.M., Micanovic, R., Galbreath, E.J., Sandusky, G.E., Hammond, L.J., Moyers, J.S., Owens, R.A., et al. (2005). FGF-21 as a novel metabolic regulator. J. Clin. Invest. *115*, 1627–1635.

Kharitonenkov, A., Wroblewski, V.J., Koester, A., Chen, Y.F., Clutinger, C.K., Tigno, X.T., Hansen, B.C., Shanafelt, A.B., and Etgen, G.J. (2007). The metabolic state of diabetic monkeys is regulated by fibroblast growth factor-21. Endocrinology *148*, 774–781.

Kunii, K., Davis, L., Gorenstein, J., Hatch, H., Yashiro, M., Di Bacco, A., Elbi, C., and Lutterbach, B. (2008). FGFR2-amplified gastric cancer cell lines require FGFR2 and Erbb3 signaling for growth and survival. Cancer Res. *68*, 2340–2348.

LeFeuvre, R.A., Rothwell, N.J., and Stock, M.J. (1987). Activation of brown fat thermogenesis in response to central injection of corticotropin releasing hormone in the rat. Neuropharmacology *26*, 1217–1221.

Lin, Z., Tian, H., Lam, K.S., Lin, S., Hoo, R.C., Konishi, M., Itoh, N., Wang, Y., Bornstein, S.R., Xu, A., and Li, X. (2013). Adiponectin mediates the metabolic effects of FGF21 on glucose homeostasis and insulin sensitivity in mice. Cell Metab. *17*, 779–789.

Lockie, S.H., Heppner, K.M., Chaudhary, N., Chabenne, J.R., Morgan, D.A., Veyrat-Durebex, C., Ananthakrishnan, G., Rohner-Jeanrenaud, F., Drucker, D.J., DiMarchi, R., et al. (2012). Direct control of brown adipose tissue thermogenesis by central nervous system glucagon-like peptide-1 receptor signaling. Diabetes *61*, 2753–2762.

Mohammadi, M., Froum, S., Hamby, J.M., Schroeder, M.C., Panek, R.L., Lu, G.H., Eliseenkova, A.V., Green, D., Schlessinger, J., and Hubbard, S.R. (1998). Crystal structure of an angiogenesis inhibitor bound to the FGF receptor tyrosine kinase domain. EMBO J. *17*, 5896–5904.

Morgan, D.A., and Rahmouni, K. (2010). Differential effects of insulin on sympathetic nerve activity in agouti obese mice. J. Hypertens. *28*, 1913–1919.

Morton, G.J., Matsen, M.E., Bracy, D.P., Meek, T.H., Nguyen, H.T., Stefanovski, D., Bergman, R.N., Wasserman, D.H., and Schwartz, M.W. (2013). FGF19 action in the brain induces insulin-independent glucose lowering. J. Clin. Invest. *123*, 4799–4808.

Nedergaard, J., Petrovic, N., Lindgren, E.M., Jacobsson, A., and Cannon, B. (2005). PPARgamma in the control of brown adipocyte differentiation. Biochim. Biophys. Acta *1740*, 293–304.

Owen, B.M., Bookout, A.L., Ding, X., Lin, V.Y., Atkin, S.D., Gautron, L., Kliewer, S.A., and Mangelsdorf, D.J. (2013). FGF21 contributes to neuroendocrine control of female reproduction. Nat. Med. *19*, 1153–1156.

Potthoff, M.J., Kliewer, S.A., and Mangelsdorf, D.J. (2012). Endocrine fibroblast growth factors 15/19 and 21: from feast to famine. Genes Dev. *26*, 312–324.

Rivier, C., Rivier, J., and Vale, W. (1986). Stress-induced inhibition of reproductive functions: role of endogenous corticotropin-releasing factor. Science *231*, 607–609.

Sarruf, D.A., Thaler, J.P., Morton, G.J., German, J., Fischer, J.D., Ogimoto, K., and Schwartz, M.W. (2010). Fibroblast growth factor 21 action in the brain increases energy expenditure and insulin sensitivity in obese rats. Diabetes *59*, 1817–1824.

Sell, H., Berger, J.P., Samson, P., Castriota, G., Lalonde, J., Deshaies, Y., and Richard, D. (2004). Peroxisome proliferator-activated receptor gamma agonism increases the capacity for sympathetically mediated thermogenesis in lean and ob/ob mice. Endocrinology *145*, 3925–3934.

Tan, B.K., Hallschmid, M., Adya, R., Kern, W., Lehnert, H., and Randeva, H.S. (2011). Fibroblast growth factor 21 (FGF21) in human cerebrospinal fluid: relationship with plasma FGF21 and body adiposity. Diabetes *60*, 2758–2762.

Thurlby, P.L., Wilson, S., and Arch, J.R. (1987). Ciglitazone is not itself thermogenic but increases the potential for thermogenesis in lean mice. Biosci. Rep. *7*, 573–577.

Véniant, M.M., Hale, C., Helmering, J., Chen, M.M., Stanislaus, S., Busby, J., Vonderfecht, S., Xu, J., and Lloyd, D.J. (2012a). FGF21 promotes metabolic homeostasis via white adipose and leptin in mice. PLoS ONE *7*, e40164.

Véniant, M.M., Komorowski, R., Chen, P., Stanislaus, S., Winters, K., Hager, T., Zhou, L., Wada, R., Hecht, R., and Xu, J. (2012b). Long-acting FGF21 has enhanced efficacy in diet-induced obese mice and in obese rhesus monkeys. Endocrinology *153*, 4192–4203.

Whittle, A.J., Carobbio, S., Martins, L., Slawik, M., Hondares, E., Vázquez, M.J., Morgan, D., Csikasz, R.I., Gallego, R., Rodriguez-Cuenca, S., et al. (2012). BMP8B increases brown adipose tissue thermogenesis through both central and peripheral actions. Cell *149*, 871–885.

Wu, A.L., Kolumam, G., Stawicki, S., Chen, Y., Li, J., Zavala-Solorio, J., Phamluong, K., Feng, B., Li, L., Marsters, S., et al. (2011). Amelioration of type 2 diabetes by antibody-mediated activation of fibroblast growth factor receptor 1. Sci. Transl. Med. *3*, ra126.

Xu, J., Lloyd, D.J., Hale, C., Stanislaus, S., Chen, M., Sivits, G., Vonderfecht, S., Hecht, R., Li, Y.S., Lindberg, R.A., et al. (2009a). Fibroblast growth factor 21 reverses hepatic steatosis, increases energy expenditure, and improves insulin sensitivity in diet-induced obese mice. Diabetes *58*, 250–259.

Xu, J., Stanislaus, S., Chinookoswong, N., Lau, Y.Y., Hager, T., Patel, J., Ge, H., Weiszmann, J., Lu, S.C., Graham, M., et al. (2009b). Acute glucose-lowering and insulin-sensitizing action of FGF21 in insulin-resistant mouse models—association with liver and adipose tissue effects. Am. J. Physiol. Endocrinol. Metab. *297*, E1105–E1114.

Zhang, Y., Breevoort, S.R., Angdisen, J., Fu, M., Schmidt, D.R., Holmstrom, S.R., Kliewer, S.A., Mangelsdorf, D.J., and Schulman, I.G. (2012). Liver LXRα expression is crucial for whole body cholesterol homeostasis and reverse cholesterol transport in mice. J. Clin. Invest. *122*, 1688–1699.